J Hepatobiliary Pancreat Surg
DOI 10.1007/s00534-009-0234-z

Interventional oncology: new options for interstitial treatments and intravascular approaches

Superselective TACE using iodized oil for HCC: rationale, technique and outcome

Osamu Matsui · Shiro Miyayama · Jyun-ichiro Sanada · Satoshi Kobayashi · Wataru Khoda · Tetsuya Minami · Kazuto Kozaka · Toshifumi Gabata

Received: 1 August 2009 / Accepted: 1 September 2009

Abstract Superselective TACE is defined as TACE from the distal portion of the feeding subsegmental hepatic artery to evoke strong ischemic effects on a small area of the liver, thus avoiding damage to liver function. Lipiodol (iodized oil) is semi-fluid, and it can flow into the surrounding portal venules and hepatic sinusoids through peribiliary plexus (PBP) and the drainage route from the hypervascular HCC. Therefore, the reversed flow from the hepatic sinusoids and portal venules to the peripheral portion of the tumor and daughter nodules can be blocked by Lipiodol injected before a particulate embolus (such as gelatin sponge particles). Common complications of superselective TACE are mild local pain and fever and temporary minimal changes of liver function. Reported CR ratio of definitely hypervascular HCC are around 30–60% by superselective TACE with Lipiodol for hypervascular HCC less than 5 cm. According to a nationwide survey by the Liver Cancer Study Group of Japan (LCSGJ), overall 5-year survival rate was 26% in patients with HCCs not indicated for surgery or RFA (PEI), mainly treated by segmental or subsegmental TACE using Lipiodol. Therefore, this TACE technique should be widely introduced as the first line technique for TACE therapy of HCC.

Keywords Hepatocellular carcinoma · TACE · Iodized oil (Lipiodol)

O. Matsui (✉) · J. Sanada · S. Kobayashi · W. Khoda · T. Minami · K. Kozaka · T. Gabata
Department of Imaging Diagnosis and Interventional Radiology, Kanazawa University Graduate School of Medical Science, Kanazawa, Japan
e-mail: matsuio@med.kanazawa-u.ac.jp

S. Miyayama
Department of Radiology, Fukui-saiseikai Hospital, Fukui, Japan

Published online: 03 November 2009

Introduction

Hepatocellular carcinoma (HCC) shows frequent multicentricity even at the time of the first diagnosis, and frequent recurrence following surgery or local ablation, especially in HCV related liver cirrhosis. In addition, it is usually associated with liver cirrhosis, and often shows intrahepatic dissemination without extrahepatic metastasis. For these multiple HCC lesions in the liver, transcatheter arterial chemoembolization (TACE) is the most important treatment method. In a 2002–2003 survey conducted by the Liver Cancer Study Group of Japan, TACE was employed in around 30% of the patients, local ablation in 31%, surgical resection in 34%, and chemotherapy in 5%, as the first line treatment for newly diagnosed HCC [1]. In addition, TACE is performed for almost all recurrent multiple HCCs. Therefore, in Japan, TACE is the most commonly performed treatment method for HCC, and an even less invasive and more effective procedure for its accomplishment would be welcomed in clinical practice.

Rationale

Superselective TACE is defined as TACE from the distal portion of the feeding subsegmental hepatic artery to evoke strong ischemic effects on a small area of the liver, thus avoiding damage to liver function ("transcatheter medical subsegmentectomy" or "transcatheter ablation" [2]).

To induce this "subsegmentectomy-like" effect, the role of Lipiodol is important. Because Lipiodol is semi-fluid, it

can flow into the surrounding portal venules and hepatic sinusoids through the peribiliary plexus (PBP) and the drainage route from the hypervascular HCC [3, 4]. According to our previous analysis, in cirrhotic livers, the PBP is markedly dilated as compared with normal liver [5]. Therefore, more Lipiodol can flow into the portal veins and hepatic sinusoids through PBP after intra-arterial injection, especially in cirrhotic livers. One of the important technical problems of TACE only with particulate embolus in HCC was the suspected reversal of flow from the surrounding hepatic sinusoids and portal venules into the peripheral portion of the tumor following TACE. Because of this flow reversal, viable cancer cells frequently remained at the tumor margin and in satellite lesions after particulate TACE without Lipiodol. On the other hand, reversed flow from the hepatic sinusoids and portal venules to the peripheral portion of the tumor and daughter nodules can be blocked by Lipiodol injected before the particulate embolus. As we reported recently [6], the strong correlation between portal vein visualization during superselective TACE and local recurrence ratio of HCC may strongly support this hypothesis.

Technique

The first indispensable step of subsegmental TACE is superselective insertion of a microcatheter into the tumoral feeding artery to treat the tumor and at least 1 cm of peritumoral safety margin of liver parenchyma. Epirubicin (EPR) is the most common anticancer drug: it is usually dissolved in non-ionic contrast medium, and then mixed with Lipiodol by pumping through a three way stopcock to make a water in oil emulsion which is stable for long hours and works as the drug carrier. The total amount of Lipiodol used is almost equal to the diameter of the tumor. The gelatin sponge sheet is cut into small cubes approximately 0.5 mm in diameter. After the administration of pentazocine, a mixture of Lipiodol and anticancer drugs is injected gradually until the abundant visualization of the surrounding portal vein and/or marked retardation of arterial flow is seen. Subsequently, gelatin sponge particles are injected until a complete stoppage of the arterial flow is achieved. In the case of multiple HCC nodules, superselective TACE is performed for each nodule.

Complications

Commonly reported complications of superselective TACE are local pain (usually mild), fever (usually mild) and temporary minimal changes of liver function. Liver failure, cholecystitis, biloma, abscess and bile duct necrosis are rare, especially if the superselective catheterization is carefully carried out [2].

Outcome

Reported CR ratios of definitely hypervascular HCC are around 30–60% by superselective TACE with Lipiodol for hypervascular HCC less than 5 cm [2, 6–8]. On the other hand, according to the reports from European RCT studies, a 15–55% of PR ratio with conventional TACE is described by Llovet et al. [9]: the discrepancy seems enormous.

Our old study showed that the overall 5- and 10-year survival rates in 172 patients with hypervascular HCC less than 4 cm in diameter and less than 3 in number treated only by superselective TACE were 50.2, and 18.5%, respectively [10]. Similar results had been reported by Matsuo et al. [11] and Takayasu et al. [8]. According to a nationwide survey by the Liver Cancer Study Group of Japan (LCSGJ) analyzing 8510 patients during 8 years [1, 12], median survival time (MST) was 34 months, and overall 5-year survival rate was 26%. 5-year survival rate increased to 52% when restricted to a subgroup with Stage I of tumor extension and liver damage A. Multivariate analysis revealed that liver damage degree, TNM stage and serum AFP value were significant prognostic factors. Although various techniques were used in this population, the majority of patients analysed were treated by superselective TACE, and procedure-related mortality was only 0.5%. These results may partly reflect the high level of confidence using TACE achieved in Japan.

Conclusions

Absolute indications of TACE are multiple HCCs, more than 3 lesions without major portal venous extension and Child-Pugh A or B, and unresectable single HCC larger than 3 cm. Relative indications are reserved for unresectable and small HCCs not amenable to thermal ablation with less than 2 lesions less than 3 cm in diameter and those patients having HCC in Child-Pugh C class cirrhosis, for whom superselective TACE is possible without significant danger.

References

1. Ikai I, Arii S, Okazaki M, et al. Report of the 17th nationwide follow-up survey of primary liver cancer in Japan. Hepatol Res. 2007;37:676–91.
2. Matsui O, Kadoya M, Yoshikawa J, et al. Small hepatocelluler carcinoma: treatment with subsegmental transcatheter arterial embolization. Radiology. 1993;188:79–83.

3. Ueda K, Matsui O, Kawamori Y, et al. Hypervascular hepatocellular carcinoma: evaluation of hemodynamics with dynamic CT during hepatic arteriography. Radiology. 1998;206:161–6.
4. Terayama N, Matsui O, Gabata T, et al. Accumulation of iodized oil within the nonneoplastic liver adjacent to hepatocellular carcinoma via the drainage routes of the tumor after transcatheter arterial embolization. Cardiovasc Intervent Radiol. 2001;24:383–7.
5. Kobayashi S, Nakanuma Y, Matsui O. Intrahepatic peribiliary vascular plexus in various hepatobiliary diseases: a histological survey. Hum Pathol. 1994;25:940–6.
6. Miyayama S, Matsui O, Yamashiro M, et al. Ultraselective transcatheter arterial chemoembolization with a 2-f tip microcatheter for small hepatocellular carcinomas: relationship between local tumor recurrence and visualization of the portal vein with iodized oil. J Vasc Interv Radiol. 2007;18:365–76.
7. Miyayama S, Mitsui T, Zen Y, et al. Histopathological findings after ultraselective transcatheter arterial chemoembolization for hepatocellular carcinoma. Hepatol Res. 2009;39:374–81.
8. Takayasu K, Muramatsu Y, Maeda T, et al. Targeted transarterial oily chemoembolization for small foci of hepatocellular carcinoma using a unified helical CT and angiography system: analysis of factors affecting local recurrence and survival rates. AJR. 2001;176:681–8.
9. Llovet JM, Real MI, Montaña X, et al. Arterial embolisation or chemoembolisation versus symptomatic treatment in patients with unresectable hepatocellular carcinoma: a randomized controlled trial. Lancet. 2002;359:1734–9.
10. Masui O, Kadoya M, Yoshikawa J, et al. Subsegmental transcatheter arterial embolization for small hepatocellular carcinoma: local therapeutic effect and 5-year survival rate. Cancer Chemother Pharmacol. 1994;33(Suppl):S84–8.
11. Matsuo N, Uchida H, Nishimine K, et al. Segmental transcatheter hepatic artery chemoembolization with iodized oil for hepatocellular carcinoma: antitumor effect and influence on normal tissue. JVIR. 1993;4:543–9.
12. Takayasu K, Arii S, Ikai I, et al. Prospective cohort study of transarterial chemoembolization for unresectable hepatocellular carcinoma in 8510 patients. Gastroenterology. 2006;131:461–9.

Cardiovasc Intervent Radiol
DOI 10.1007/s00270-009-9697-1

CLINICAL INVESTIGATION

The March of Extrahepatic Collaterals: Analysis of Blood Supply to Hepatocellular Carcinoma Located in the Bare Area of the Liver After Chemoembolization

Shiro Miyayama · Masashi Yamashiro · Miho Okuda · Yuichi Yoshie · Yoshiko Nakashima · Hiroshi Ikeno · Nobuaki Orito · Osamu Matsui

Received: 16 May 2009 / Accepted: 11 August 2009

Abstract The purpose of this study was to evaluate changes in vascular supply to hepatocellular carcinoma (HCC) located in the bare area of the liver in patients who were mainly treated with chemoembolization. Twenty-six patients with HCC showing a mean diameter of 3.1 ± 1.4 cm (mean ± standard deviation) were mainly treated with chemoembolization. All patients underwent 2.7 ± 2.3 chemoembolization sessions over 40.1 ± 25.2 months. Tumor feeding branches demonstrated in each chemoembolization session were retrospectively evaluated. Initially, 18 tumors (59.2%) were supplied by the hepatic artery (H) and 8 (30.8%) by both the hepatic and the extrahepatic arteries (H + C). Fourteen tumors (53.8%) recurred at the posterior aspect of the tumor and were supplied by H ($n = 4$), H + C ($n = 5$), and extrahepatic collaterals (C) ($n = 5$). Several tumors recurred despite repeated chemoembolization, and these were supplied by H ($n = 1$), H + C ($n = 7$), and C ($n = 2$) at the second recurrence, by H ($n = 1$), H + C ($n = 2$), and C ($n = 3$) at the third, by H + C ($n = 2$) and C ($n = 2$) at the fourth, by H + C ($n = 2$) and C ($n = 2$) at the fifth, and by H ($n = 1$) and C ($n = 1$) at the sixth. One tumor was supplied by H at the seventh and by H + C at the eighth recurrence. As the number of local recurrences increased, the feeding vessel shifted from H to C. Especially, the right inferior phrenic artery (IPA) and renal capsular artery (RCA) supplied the tumor early, while the small right RCAs, adrenal arteries, and intercostal and lumbar artery supplied late recurrences in turns. In conclusion, HCCs located in the bare area are frequently supplied by extrahepatic vessels initially, while recurrence after chemoembolization is mainly due to extrahepatic blood supply. The right IPA and RCA are common feeding vessels demonstrated early, while other extrahepatic collateral supply from the retroperitoneal circulation occurs in turns during the later course.

Keywords Hepatocellular carcinoma · Chemoembolization · Bare area of the liver · Extrahepatic blood supply

S. Miyayama (✉) · M. Yamashiro · M. Okuda · Y. Yoshie · Y. Nakashima · H. Ikeno · N. Orito
Department of Diagnostic Radiology, Fukuiken Saiseikai Hospital, 7-1, Funabashi, Wadanaka-cho, Fukui 918-8503, Japan
e-mail: s-miyayama@fukui.saiseikai.or.jp

O. Matsui
Department of Radiology, Kanazawa University Graduate School of Medical Science, 13-1, Takara-machi, Kanazawa 920-8641, Japan

Introduction

Hepatocellular carcinoma (HCC) frequently recurs after chemoembolization and development of extrahepatic collateral pathways is one of the causes of local tumor recurrence. Several extrahepatic collateral pathways supplying HCC have been reported [1–14].

At the level of the bare area of the liver, branches of the inferior phrenic arteries (IPAs) are in direct contact with the liver [3, 4]. In the event of hepatic artery damage, or even with a patent hepatic artery, these branches contribute substantially to the hepatic tumor vascular supply. In addition, IPAs usually anastomose with several arteries, such as the internal mammary artery and intercostal arteries [5, 6, 15]. Therefore, a tumor located in the bare area of the liver has the potential to receive collateral blood flow through several individual sources. Extrahepatic collateral supplies can inhibit the effectiveness of chemoembolization. For transcatheter management of HCC to be effective, these collaterals should be adequately embolized [1–14].

Published online: 12 September 2009

Therefore, interventional radiologists should have sufficient knowledge of extrahepatic blood supply to HCCs.

In this report, we retrospectively analyzed changes in vascular supply to HCCs located in the bare area of the liver during the subsequent clinical course of patients who were mainly treated by chemoembolization.

Materials and Methods

Patients

In the present study, we define "the bare area of the liver" as the posterior surface of Segment 7 demarcated by the right hepatic vein. Although we are well aware that "the bare area of the liver" also includes a part of lateral surface of Segment 8, the right-side margin is not anatomically outlined clearly. Between August 1999 and August 2008, we treated 26 consecutive HCC lesions in the bare area of the liver by chemoembolization. The patient profiles are summarized in Table 1. There were 14 men and 12 women and the mean patient age was 68.9 ± 7.5 years (mean ± standard deviation; range, 51 to 81 years). All patients had liver cirrhosis, which was associated with hepatitis C in 19 patients and hepatitis B in 6 patients, while in the remaining patient, the etiology was unknown. All patients had a single HCC lesion at the bare area, including 6 patients with 1 other HCC in addition to the tumor in the bare area and 2 patients with multiple HCCs but fewer than 5 lesions at other sites. The mean diameter of tumors in the bare area was 3.1 ± 1.4 cm (range, 1–6 cm). Diagnosis was established by imaging findings on computed tomography (CT) and/or magnetic resonance (MR) imaging, characteristic nodular enhancement during the arterial phase, and washout during the delayed phase images in all patients.

Initially, 22 tumors were treated by chemoembolization alone and 4 were treated by a combination of chemoembolization and radiofrequency ablation (RFA).

Table 1 Patent profiles

Patient characteristic	
Gender	
Male	14
Female	12
Mean age (yr)	68.9 ± 7.5
Liver cirrhosis	26 (100%)
HCV related	19 (73.1%)
HB related	6 (23.1%)
Etiology unknown	1 (3.8%)
Tumor size in the bare area (cm)	3.1 ± 1.4
Intrahepatic multiplicity	
Single	18 (69.2%)
Two	6 (23.1%)
Three-5 lesions	2 (7.7%)
Treatment	
Chemoembolization alone	22 (84.6%)
Combination of chemoembolization & RFA	4 (15.4%)

RFA radiofrequency ablation

Chemoembolization Procedure

Written informed consent was obtained from each patient before the chemoembolization and RFA procedures. Institutional review board approval was not required at our institution for this retrospective study.

A 2-Fr tip (Progreat α; Terumo, Tokyo, Japan) was mainly used for all chemoembolization procedures. To navigate the microcatheter, a 0.016-in. guidewire (GT-wire; Terumo) was used. After the microcatheter was inserted into the feeding branch, 0.5 ml of 2% lidocaine (Xylocaine; Fujisawa, Osaka, Japan) was intra-arterially injected to prevent pain and vasospasm. First, a mixture of iodized oil (Lipiodol; Andre Guerbet, Aulnaysous-Bois, France) and anticancer drugs (epirubicin [Farmorbicin], Kyowa Hakko, Tokyo, Japan; mitomycin C [Mitomycin], Kyowa Hakko) was injected, and injection of gelatin sponge particles followed. Until December 2006, gelatin sponge particles (Gelfoam; Upjohn, Kalamazoo, MI, USA) cut into approximately 1-mm cubes were used. Since January 2007, 1-mm-diameter commercially available gelatin sponge particles (Gelpart; Nippon Kayaku, Tokyo, Japan) were used.

The embolized branches of the hepatic artery were minimized as selectively as possible in each patient. Extrahepatic collaterals were searched for with the use of a 4-Fr shepherd-hook catheter (Terumo) or cobra-shaped catheter (Hanako Medical, Kobe, Japan). When tumor stain was demonstrated through the extrahepatic vessel on angiography, the tumor-feeding branch was selected by the microcatheter. In total, 1–6 ml of iodized oil, 10–30 mg of epirubicin, and 2–6 mg of mitomycin C were used in a single chemoembolization session, depending on the size of each tumor.

RFA Procedure

RFA was performed 1–2 weeks after chemoembolization in the first 4 consecutive tumors (2.5–5 cm in diameter; mean, 3.3 ± 1.4 cm) in 4 patients. The procedure was performed using an expandable electrode (LeVeen; Radiotherapeutics, Sunnyvale, CA, USA) under ultrasonographic (US) guidance without injection of saline into the pleural cavity. However, RFA was not performed after the fifth patient because we were able to obtain a complete ablative margin in only 1 of the previous 4 tumors.

Follow-Up

Unenhanced CT was obtained 1 week after chemoembolization in all patients to check for iodized oil accumulation within the target tumor. In addition, dynamic CT was also performed the day after RFA. All patients were followed with dynamic CT and/or MR imaging obtained every 2–3 months after treatment to screen for any tumor recurrence. When tumor recurrence and/or newly developed tumors at other sites were detected, additional chemoembolization was performed, if possible.

Definition of Extrahepatic Collateral Supply to HCC

Several extrahepatic collaterals were searched when extrahepatic blood supply to the tumor was suspected. Initial extrahepatic blood supply to HCC was defined as follows: (i) an obvious tumor stain was demonstrated on arteriogram of the extrahepatic vessel during the initial chemoembolization; and (ii) arteriogram of the extrahepatic vessel during additional chemoembolization showed a stain corresponding to the tumor area that had not shown accumulation of iodized oil on CT obtained 1 week after the initial chemoembolization despite the lack of an obvious extrahepatic supply to HCC during the initial procedure (including cases that did not undergo arteriogram of extrahepatic vessels). Extrahepatic blood supply to recurrent HCC was confirmed when tumor stain was demonstrated on arteriogram of extrahepatic collaterals.

Definition of Tumor Recurrence

The tumor portion where iodized oil was not accumulated after the initial chemoembolization was defined as a "residual portion," not a "recurrent portion." Tumor recurrence was defined as the development of a viable tumor portion after the entire tumor was embolized by the initial or additional chemoembolization. The interval between the initial chemoembolization and the demonstration of recurrence on CT or MR imaging was defined as the period of tumor control.

Results

Findings at the Initial Chemoembolization

All tumors were partially or completely supplied by the hepatic arterial branches at the initial chemoembolization. The embolized hepatic artery was the superior posterior subsegmental artery (A7) ($n = 12$), posterior segmental artery ($n = 7$), superior anterior subsegmental artery (A8) and A7 ($n = 5$), inferior posterior subsegmental artery (A6) ($n = 1$), and A7 and the caudate artery ($n = 1$).

Arteriograms of extrahepatic collateral vessels were obtained in 18 patients (69.2%) during the initial chemoembolization procedure. Arteriogram of the right IPA was obtained in 12 patients, right IPA and right renal capsular artery (RCA) in 5, and right RCA and right middle adrenal artery in 1. In 2 patients, the right IPA was reconstructed through the dorsal pancreatic artery arising from the superior mesenteric artery ($n = 1$) or left gastric artery ($n = 1$) (Fig. 1). One right IPA could not be detected during the initial chemoembolization procedure because a vessel that arose from the left renal polar artery was demonstrated at the second chemoembolization when it was shown to supply the tumor (Fig. 2). Extrahepatic blood supply to the tumor at the initial procedure was observed in 8 tumors (30.8%), with a mean tumor diameter of 3.4 ± 1.4 cm (range, 1.6–6 cm), through the right IPA ($n = 5$), right IPA and right RCA ($n = 2$), and right RCA ($n = 1$). In 5 tumors, the extrahepatic collateral supply was demonstrated during the initial procedure and chemoembolization through these feeding branches was subsequently performed. In the remaining 3 tumors supplied by the right IPA ($n = 2$) and right RCA ($n = 1$), arteriograms of these vessels were not obtained during the initial procedure. Based on CT findings obtained 1 week after the procedure that showed a tumor area without iodized oil accumulation, additional chemoembolization was performed through these vessels 2–3 months after the initial chemoembolization.

Tumor Recurrence After Treatment

All patients were followed for a mean of 40.1 ± 25.2 months (range, 8–116 months). In all 26 tumors, including 3 tumors that were treated with additional chemoembolization sessions, iodized oil was accumulated in the entire tumor. In 3 of 4 tumors treated with RFA after chemoembolization, the ablative area did not cover the entire tumor on CT and these tumors recurred at 14.3 ± 5.5 months (range, 9–20 months). In total, 14 tumors (53.8%), 11 of 22 tumors treated by chemoembolization alone and 3 of 4 tumors treated by a combination of chemoembolization and RFA, recurred 13.2 ± 9.0 months (range, 4–40 months) after the initial treatment. All 14 tumors recurred at the posterior aspect of the tumor arising in the bare area. Second recurrence was observed in 10 tumors 6.5 ± 3.1 months (range, 2–12 months) after treatment. Despite repeated chemoembolization, third recurrence was observed in 7 tumors after 5.7 ± 2.6 months (range, 3–11 months), fourth recurrence was observed in 6 tumors after 5.3 ± 2.2 months (range, 4–8 months), fifth recurrence was observed in 4 tumors after 9.8 ± 6.4 months (range, 5–19 months), and sixth recurrence was observed in 3 tumors after 4.7 ± 3.8 months (range, 2–9 months). Moreover, 1 tumor recurred at 10, 23, and 5 months after each additional

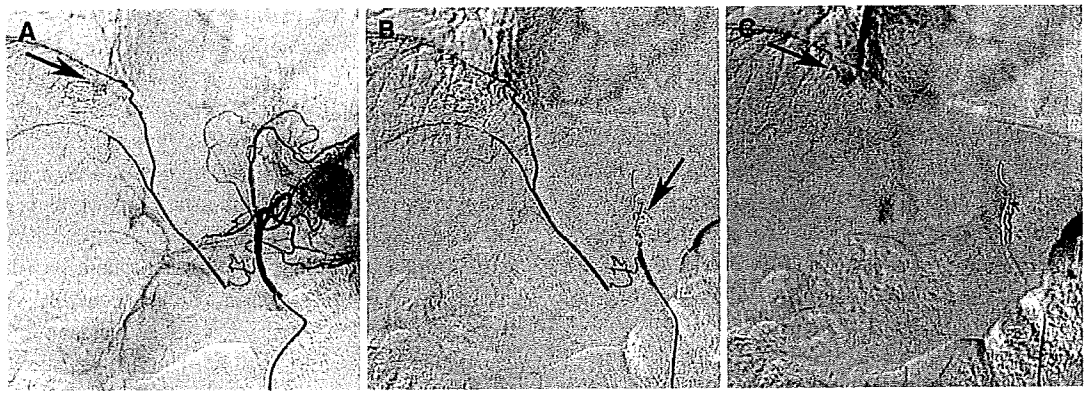

Fig. 1 A 76-year-old man with a recurrent HCC located in the bare area of the liver after chemoembolization through the hepatic arterial branch. **A** Arteriogram of the left gastric artery shows the reconstructed right IPA and tumor stain (*arrow*). **B** The anasotomosis branch could not be selected, therefore embolization of the left gastric artery at the distal end from the anastomosis branch was performed, using metallic coils (*arrow*). **C** The tumor stain (*arrow*) is clearly depicted, without gastric wall staining after coil embolization. Chemoembolization was successfully performed, without any complications, through the left gastric artery

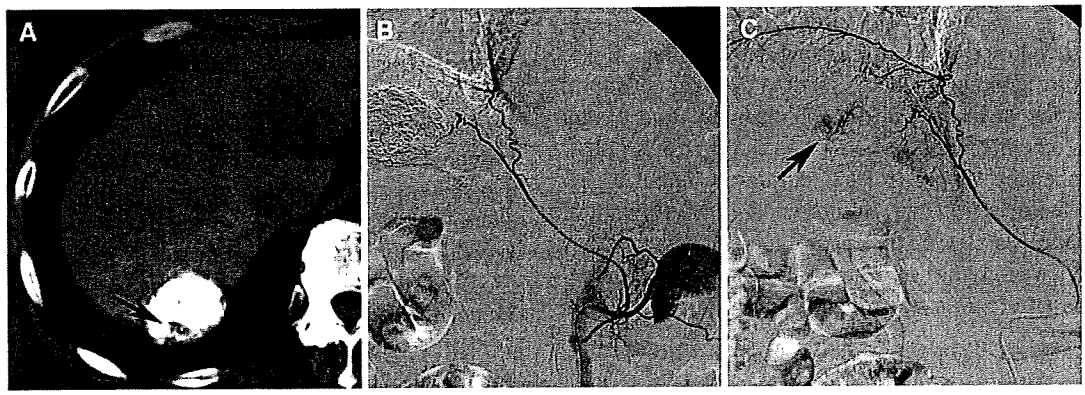

Fig. 2 A 68-year-old man with an HCC located in the bare area of the liver. **A** CT obtained 1 week after chemoembolization through the hepatic arterial branch shows a defect of iodized oil accumulation at the posterior aspect of the tumor (*arrow*). **B** The right IPA is derived from the left upper renal polar branch. **C** Selective arteriogram of the right IPA shows a tumor stain corresponding to the defect of iodized oil (*arrow*)

chemoembolization session and the tumor was finally treated by irradiation. In total, 19 tumors (73.1%) could be controlled but 7 (26.9%) could not, despite repeated chemoembolization. Nine patients died after 42.9 ± 15.1 months (range, 18–69 months), including 3 who died of liver-unrelated causes (pneumonia [$n = 1$], traffic accident [$n = 1$], and pancreatic cancer [$n = 1$]). To date, 17 patients have survived 37.5 ± 29.0 months (range, 8–116 months) after the initial treatment, including 1 patient with a recurrent tumor in the bare area and 2 patients with a viable tumor at another site.

Extrahepatic Collateral Supply to Recurrent Tumors

All patients underwent 1–10 chemoembolization sessions (mean, 2.7 ± 2.3 sessions) for HCC in the bare area. During the subsequent treatment course, arteriogram of the right IPA was obtained for all but 1 patient (96.2%) whose tumor did not recur after the initial chemoembolization procedure. Arteriogram of the right RCA was obtained in 21 patients (80.8%), except for 4 patients without tumor recurrence after the initial chemoembolization and 1 patient whose recurrent tumor after the initial chemoembolization was controlled by chemoembolization through the right IPA. Arteriogram of the right intercostal and/or lumbar artery was obtained in 9 patients (34.6%), and arteriogram of the adrenal arteries directly arising from the aorta was obtained in 7 patients (26.9%). In 1 patient (3.8%), arteriogram of the right gonadal artery directly arising from the aorta was also obtained.

During follow-up, extrahepatic collateral supply to the tumor was observed in 18 patients (69.2%), including 8 (30.8%) in whom findings were observed at the initial treatment (Table 2). The tumor-feeding extrahepatic

Table 2 Incidence of blood supply to HCCs from extrahepatic collaterals

	During follow-up (n = 18; 69.3%)	At initial treatment (n = 8; 30.8%)
RIPA	13	7
RRCA	7	3
RMAA	4	
RIAA	4	
RLA	4	
RICA	2	
DPA	1	
BDA	1	

RIPA right inferior phrenic artery, *RRCA* right renal capsular artery, *RMAA* right middle adrenal artery, *RIAA* right inferior adrenal artery, *RICA* right posterior intercostal artery, *RLA* right lumbar artery, *DPA* dorsal pancreatic artery, *BDA* bile duct artery

collateral was the right IPA (n = 13), right RCA (n = 7), right middle adrenal artery (n = 4), right lumbar artery (n = 4), right inferior adrenal artery (n = 4), right intercostal artery (n = 2), bile duct artery (n = 1), and dorsal pancreatic artery (n = 1). All tumor-feeding branches were embolized during each procedure. One feeding branch derived from the left gastric artery connected with the reconstructed right IPA could not be directly selected because of its small caliber and acute angulation. The left gastric artery was embolized using metallic coils (Tornado; Cook, Bloomington, IN, USA) at the distal level of the anastomosis branch to prevent nontarget embolization, and chemoembolization was successfully performed through the microcatheter placed in the left gastric artery proximal to the anastomosis branch (Fig. 1).

Change of the Feeding Vessel in Each Recurrence

At the initial chemoembolization, 18 tumors (69.2%) were supplied by the hepatic artery alone and 8 (30.8%) were supplied by both the hepatic and the extrahepatic arteries. Of 14 tumors showing first recurrence, 4 tumors were supplied by the hepatic artery, 5 were supplied by both the hepatic and the extrahepatic arteries, and 5 were supplied by extrahepatic collaterals alone. Of 10 tumors showing second recurrence, 1 tumor was supplied by the hepatic artery alone, 7 were supplied by both the hepatic and the extrahepatic arteries, and 2 were supplied by extrahepatic collaterals alone. In 6 of 7 tumors showing third recurrence, 1 tumor was supplied by the hepatic artery alone, 2 were supplied by both the hepatic and the extrahepatic arteries, and 3 were supplied by extrahepatic collaterals alone. Angiography was not performed for the remaining tumor because of poor hepatic function. In 4 of 6 tumors showing fourth recurrence, 2 tumors were supplied by both

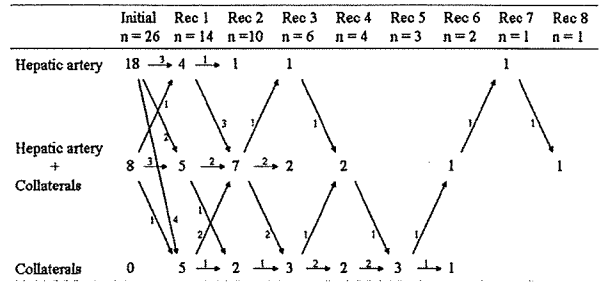

Fig. 3 Changes in blood supply to recurrent tumors. As the number of tumor recurrences increases, the tumor-feeding vessels shift from the hepatic artery to the extrahepatic collaterals

the hepatic and the extrahepatic arteries and 2 were supplied by extrahepatic collaterals alone. Angiography was not performed for the remaining 2 tumors because of poor hepatic function or dementia. In 3 of 4 tumors showing fifth recurrence, all tumors were supplied by extrahepatic collaterals alone. Angiography was not performed for the remaining tumor because of diffuse metastases. In 2 of 3 tumors showing sixth recurrence, 1 was supplied by both the hepatic and the extrahepatic arteries and 1 was supplied by extrahepatic collaterals alone. Angiography was not performed for 1 tumor because of diffuse metastases. At the seventh recurrence, the tumor was again supplied by the restored hepatic artery, and it was supplied by both the hepatic and the extrahepatic arteries at the eighth recurrence. As the number of tumor recurrences increased, the tumor-feeding vessels shifted from the hepatic artery to extrahepatic collaterals (Fig. 3). Table 3 shows the tumor-feeding branches at each recurrence in patients who underwent 3 or more chemoembolization procedures. In particular, other or small right RCAs, right adrenal arteries, and right lumbar and intercostal arteries fed the tumor in turns after the right IPA or right RCA had already been embolized (Figs. 4, 5, 6).

Discussion

Extrahepatic collateral pathways to the liver and HCC are established under various conditions. These pathways mainly develop after interruption of the hepatic artery by surgical ligation, arterial injury induced by repeated chemoembolization procedures, or placement of a catheter. Adhesion between the liver and the other organ exaggerates the degree of extrahepatic collaterals [7]. An extrahepatic blood supply to HCC also develops in the anatomical location of a tumor, although the hepatic arterial supply remains intact [3, 14]. In particular, it is thought that extrahepatic collateral supplies develop early in the bare area of the liver [14].

Table 3 Changes in tumor-feeding vessels of HCCs located in the bare area of the liver in patients who underwent three or more chemoembolization sessions

Patient no./age/gender	Initial	Rec 1	Rec 2	Rec 3	Rec 4	Rec 5	Rec 6	Rec 7	Rec 8	Duration
1/68/M		A7	A7	Post Br						1 years 3 months
	RIPA	RIPA	RICA							
	RRCA	RMAA								
2/73/M	A7	A7	A7	A7	RIPA	RRCA [2]	RLA	A7	A7	9 years 2 months
			RIPA	RRCA [1]	RIAA	RIAA			RRCA [3]	
3/68/F	A7	A7	A7	Post Br						2 years 5 months
	RRCA [1]		RIAA [1, 2]	RRCA [2–4]						
				RLA						
4/63/F	A7	RIPA	A7	Post Br	RIPA	RIPA				4 years 1 months
			RIPA	RIPA	RRCA [2]	RRCA [3, 4]				
				RRCA [1]		RIAA				
				RICA		RICA				
						RLA				
5/76/M	A7	RIPA	RIPA							1 years 2 months
			RMAA							
6/76/F	Post Br	Post Br	A7							1 years 8 months
7/71/F	Post Br	PIPA	A7	RLA						2 years 2 months
			RIPA							
8/73/F	Post Br	RIPA	A7							4 months
			RIPA							
9/77/F	A7	Post Br	Post Br	Post Br						2 years 2 months
				RIPA						
10/59/M	Post Br	Post Br	RIPA	RIPA	RMAA	RIAA [1]	Post Br			3 years 2 months
		A1	RRCA			DPA	A1			
		RIPA					BDA			
							RIAA [2]			
11/76/M	A7	A7	A7							9 months
		A8	A8							
		RIPA	RIPA							

Rec recurrence, *Post Br* posterior segmental artery of the right hepatic artery, *RIPA* right inferior phrenic artery, *RRCA* right renal capsular artery, *RMAA* right middle adrenal artery, *RICA* right posterior intercostal artery, *RIAA* right inferior adrenal artery, *RLA* right lumbar artery, *DPA* dorsal pancreatic artery, *BDA* bile duct artery

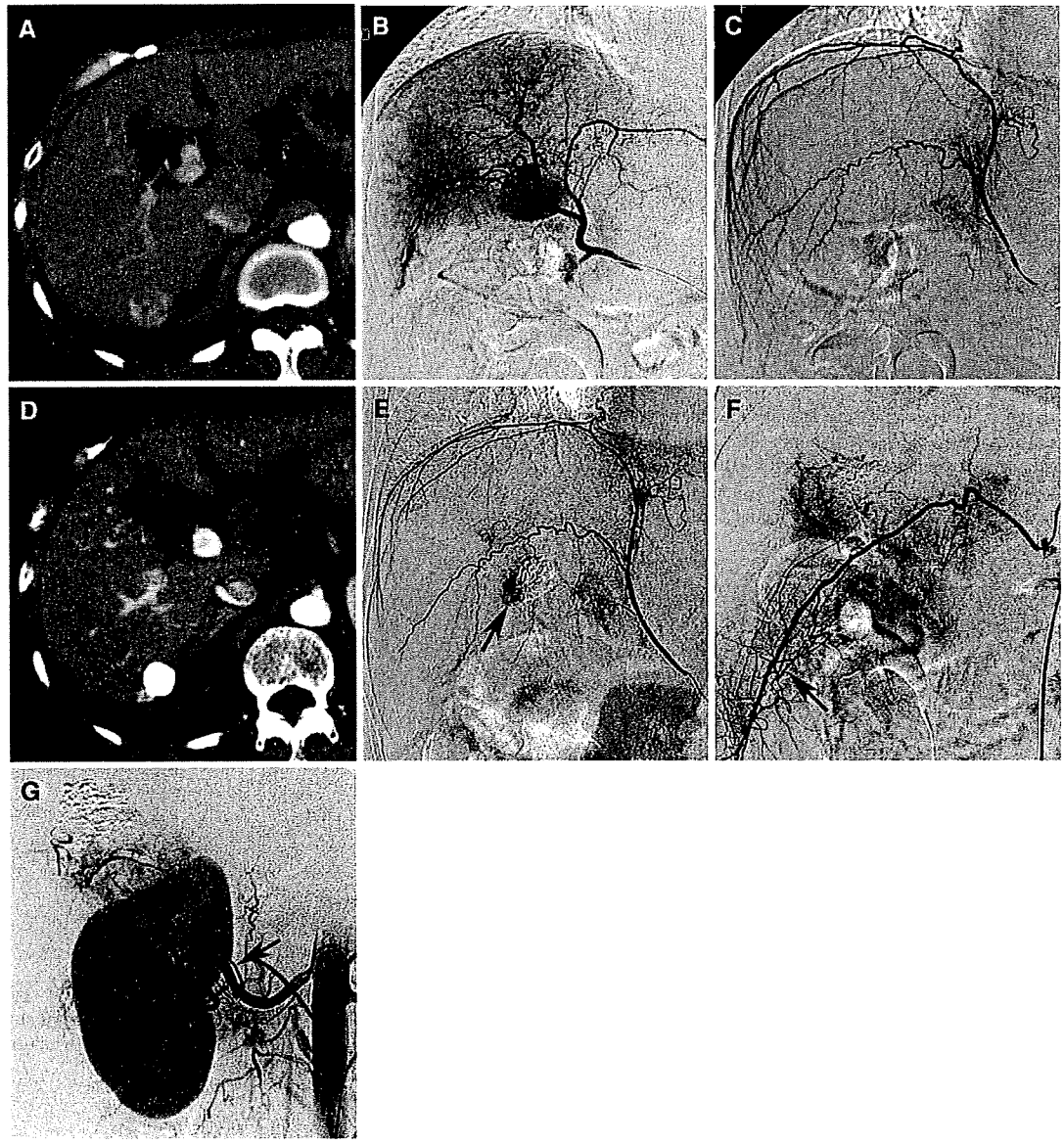

Fig. 4 A 63-year-old woman with an HCC located in the bare area of the liver. **A** Arterial phase CT shows an enhancing tumor in the bare area of the liver. **B** Arteriogram of the proper hepatic artery shows tumor stain supplied by the posterior superior subsegmental artery of the liver. The branch was selected and chemoembolization was performed. **C** Arteriogram of the right IPA obtained simultaneously during the initial chemoembolization does not show any tumor stains. In this patient, RFA was added after chemoembolization. **D** CT obtained 20 months after the initial treatment shows a recurrent tumor (*arrow*). **E** Arteriogram of the right IPA shows a tumor stain in turn (*arrow*). Chemoembolization was performed; however, the tumor recurred again after treatment. **F** At the third recurrence (2 years 11 months after the initial treatment), the tumor is supplied by the right 11th intercostal artery. The tumor-feeding branch (*arrow*) was selected and chemoembolization was performed. The posterior branch of the right hepatic artery, right IPA, and right RCA were simultaneously embolized (not shown). **G** At the fourth recurrence (3 years 4 months after the initial treatment), the tumor is supplied by another right RCA (*arrow*), in addition to the right IPA supply

The right IPA is the major source of diaphragmatic pathways and is the most frequent extrahepatic collateral vessel of HCCs [12–14]. There is close contact between the posterior portion of the liver and the diaphragm in the bare area, and branches of the IPA are in direct contact with the liver [3, 4]. Takeuchi et al. [16] clearly demonstrated blood supply to the liver from the right IPA immediately after balloon occlusion of the proper hepatic artery using a unified CT and angiography system. Chung et al. [3] also reported that right IPA parasitization was retrospectively

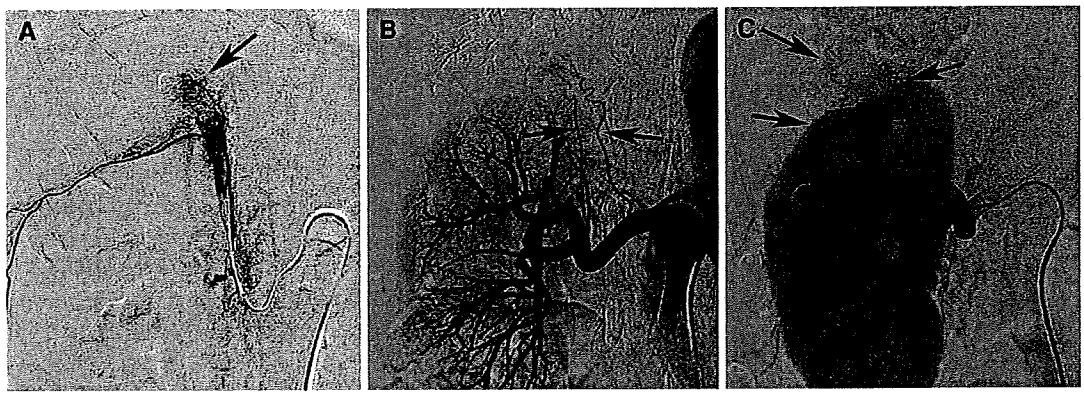

Fig. 5 A 68-year-old woman with an HCC located in the bare area. **A** At the initial treatment, the residual tumor after chemoembolization of the hepatic arterial branch (*arrow*) is fed by the right RCA. **B** The recurrent tumor 1 year after the procedure is supplied by the hepatic arterial branch (not shown). At the second recurrence (1 year 8 months after the initial treatment), the tumor is fed by two right inferior adrenal arteries (*arrows*). Chemoembolization was performed through these vessels. **C** At the third recurrence (2 years 5 months after the initial treatment), the tumor is fed by 3 small RCAs (*arrows*)

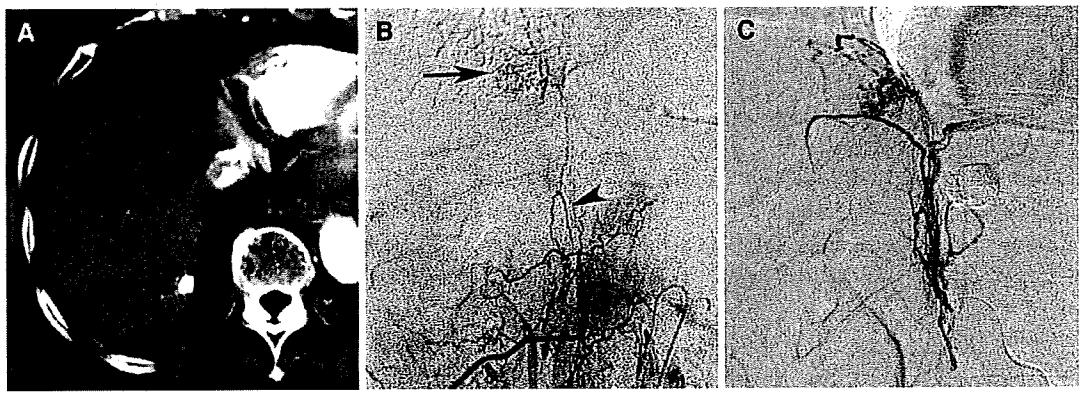

Fig. 6 A 71-year-old woman with an HCC located in the bare area. **A** Arterial phase CT at the third recurrence 4 years 2 months after the initial treatment shows a tumor protruding to the bare area (*arrow*). **B** The tumor was initially supplied by the hepatic arterial branch and was supplied by the right IPA at the first and second recurrences (not shown). At the third recurrence, the tumor (*arrow*) is supplied by a small branch arising from the right first lumbar artery (*arrowhead*). **C** The tumor-feeding branch was selected and chemoembolization was successfully performed

suspected at the initial chemoembolization in 80% of their patients, with blood supply to tumors from the right IPA demonstrated on follow-up angiography.

The RCA system distributes to the renal capsule and perirenal space, and it is composed of three basic pathways: superior, medial, and inferior RCAs. These vessels usually arise from or together with the adrenal arteries. The system may also originate from the main renal artery or from the gonadal artery. In addition, perforating capsular arteries (small RCAs) arise from the arcuate and interlobular arteries, which are branches of the renal artery [17]. The perirenal space is anatomically connected with the bare area on the right side [18], therefore, the right RCA also distributes into the bare area.

The intercostal artery and internal mammary artery usually connect with the right IPA and support the diaphragmatic pathways [5]. There are also fine retroperitoneal networks between the right IPA, right RCA, dorsal pancreatic artery, adrenal artery, left gastric artery, and right lumbar artery [6]. Therefore, these vessels also infrequently act as a supportive diaphragmatic pathway [5, 19]. Because of such overlapping vascular territories, a tumor located in the bare area may potentially be fed by several separate extrahepatic collateral vessels, in addition to the hepatic arterial branch. When one vessel is attenuated by chemoembolization, other vessels may in turn replace the blood supply to the recurrent tumor at the next chemoembolization session. We named this sequence "the march of extrahepatic collaterals" (Fig. 7).

As the tumor size increases, the prevalence of an extrahepatic supply increases [13]. Chung et al. [14] reported that prevalence of extrahepatic blood supply at the initial chemoembolization session in a tumor <4 cm in

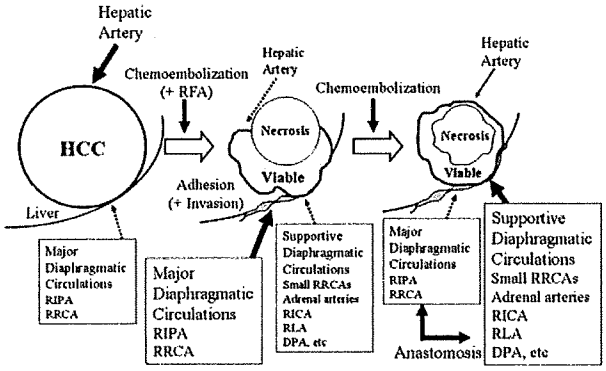

RIPA right inferior phrenic artery, *RRCA* right renal capsular artery, *RICA* right intercostal artery, *RLA* right lumbar artery, *DPA* dorsal pancreatic artery

Fig. 7 Schematic representation of "the march of extrahepatic collaterals." At the beginning of the treatment, the tumor located in the bare area of the liver is mainly supplied by the hepatic arterial branch and partially supplied by major extrahepatic collaterals, such as the right IPA and right RCA. After damage to these vessels by repeated chemoembolization, minor extrahepatic collateral vessels of retroperitoneal circulation, such as the small right RCAs, adrenal arteries, posterior intercostal artery, and lumbar artery, feed the recurrent tumor in turns

diameter was <3%; this increased to 63% when the tumor was >6 cm in diameter. In the present study, however, 30.8% of tumors with a mean diameter of 3.4 cm were receiving an extrahepatic blood supply at the initial chemoembolization. This suggests that extrahepatic parasitization easily develops even for a small tumor located in the bare area.

At the beginning of treatment, a tumor located in the bare area of the liver was mainly supplied by the hepatic arterial branch and partially supplied by major extrahepatic collaterals, such as the right IPA and right RCA. After damage to these vessels by repeated chemoembolization, minor extrahepatic collateral vessels of the retroperitoneal circulation, such as small right RCAs, adrenal arteries, posterior intercostal artery, and lumbar artery, fed the recurrent tumor in turns. Adhesion between the liver and the diaphragm after repeated chemoembolization and RFA may also exaggerate the development of such minor extrahepatic collaterals. These small vessels may make it more difficult to control the tumor by chemoembolization after the tumor has recurred several times.

RFA is one of the most effective techniques for local treatment of inoperable HCCs. It is also useful to treat a tumor located in the bare area, however, several thoracic complications, such as diaphragmatic perforation (intrathoracic hernia, abscess extending to the thorax, and bronchobiliary fistula), right shoulder pain, and pleural effusion, have been reported [20–22]. In a report by Kang et al. [22], RFA of a tumor abutting the diaphragm was less effective with regard to technical success and local tumor control because of the difficulty in targeting the tumor by US. In addition, the operator's concern regarding thermal injury of the adjacent diaphragm may lead to incomplete ablation because it is very difficult to monitor the ablative zone and the diaphragm in the subphrenic area with a poor sonic window and ill-defined hyperechoic zone during ablation. Conversely, Takaki et al. [23] reported that there was no significant difference in tumor progression rates between tumors adjacent to the diaphragm and tumors apart from the diaphragm after CT-guided RFA combined with chemoembolization. In our small number of patients treated with a combination of chemoembolization and US-guided RFA, however, the ablative margin did not cover the entire tumor in 3 of 4 cases, and these 3 tumors subsequently recurred. CT guidance may allow the operator to easily target tumor abutting the diaphragm by the RF electrode, although the risk of thermal injury to the diaphragm remains [21].

Local recurrence rates of HCCs located in the bare area treated with chemoembolization were higher than those of HCCs treated with RFA in a report by Kang et al. [22]. We speculate that differences in local recurrence rates in each study may involve a different tumor location rather than different therapeutic modalities. In the present study, all tumors were located in the bare area. However, in their report, not only tumors abutting the diaphragm but also tumors located within a 5-mm-wide area near the diaphragm were included in the "abutting group." In addition, the hepatic segment of the tumor location was not provided. We speculate that tumors originating in the bare area may be more difficult to treat by a combination of chemoembolization and RFA than tumors in other segments abutting the diaphragm.

There are some limitations to the present study. We excluded equivocal staining on angiograms of extrahepatic collaterals. In addition, in elderly patients with atherosclerosis, screening of small branches arising directly from the aorta, such as the middle adrenal artery, may be incomplete. For these reasons, the incidence of blood supply from extrahepatic collaterals to the tumor may have been underestimated in this study. In addition, "tumor recurrence" in the present study may include small residual tumor tissue following the initial or additional chemoembolization. Therefore, the prevalence of extrahepatic blood supply to HCC at the initial chemoembolization may also have been underestimated.

In conclusion, HCCs located in the bare area are frequently supplied by extrahepatic vessels in addition to the hepatic artery even at the initial treatment. Recurrence of such tumors after chemoembolization is mainly due to the extrahepatic blood supply. The right IPA and RCA are common feeding vessels demonstrated early, while other extrahepatic collateral supply from the retroperitoneal circulation, such as the small right RCAs, adrenal arteries,

and intercostal and lumbar artery, occurs in turns during the later course. Interventional radiologists should be familiar with the clinical features of HCCs located in the bare area and the complex vascular sequence supplying such tumors.

References

1. Kim JH, Chung JW, Han JK et al (1995) Transcatheter arterial embolization of the internal mammary artery in hepatocellular carcinoma. J Vasc Interv Radiol 6:71–74
2. Nakai M, Sato M, Kawai N et al (2001) Hepatocellular carcinoma: involvement of the internal mammary artery. Radiology 219:147–152
3. Chung JW, Park JH, Han JK et al (1998) Transcatheter oily chemoembolization of the inferior phrenic artery in hepatocellular carcinoma: the safety and potential therapeutic role. J Vasc Interv Radiol 9:495–500
4. Duprat G, Charnsangavej S, Wallace S et al (1998) Inferior phrenic artery embolization in the treatment of hepatic neoplasms. Acta Radiol 29:427–429
5. Park SI, Lee DY, Won JY et al (2003) Extrahepatic collateral supply of hepatocellular carcinoma by the intercostal arteries. J Vasc Interv Radiol 14:461–468
6. Miyayama S, Matsui O, Taki K et al (2004) Transcatheter arterial chemoembolization for hepatocellular carcinoma fed by the reconstructed inferior phrenic artery: anatomical and technical analysis. J Vasc Interv Radiol 15:815–823
7. Miyayama S, Matsui O, Akakura Y et al (2001) Hepatocellular carcinoma with blood supply from omental branches: treatment with transcatheter arterial embolization. J Vasc Interv Radiol 12:1285–1290
8. Kodama Y, Shimizu T, Endo H et al (2002) Spontaneous rupture of hepatocellular carcinoma supplied by the right renal capsular artery treated by transcatheter arterial embolization. Cardiovasc Intervent Radiol 25:137–140
9. Miyayama S, Matsui O, Nishida H et al (2003) Transcatheter arterial chemoembolization for unresectable hepatocellular carcinoma fed by the cystic artery. J Vasc Interv Radiol 14:1155–1161
10. Suh SH, Won JY, Lee DY et al (2005) Chemoembolization of the left inferior phrenic artery in patients with hepatocellular carcinoma: radiologic findings and clinical outcome. J Vasc Interv Radiol 16:1741–1745
11. Kim HC, Chung JW, Jae HJ et al (2006) Hepatocellular carcinoma: transcatheter arterial chemoembolization of the gonadal artery. J Vasc Interv Radiol 17:703–709
12. Kim HC, Chung JW, Lee W et al (2005) Recognizing extrahepatic collateral vessels that supply hepatocellular carcinoma to avoid complications of transcatheter arterial chemoembolization. Radiographics 25:S25–S39
13. Miyayama S, Matsui O, Taki K et al (2006) Extrahepatic blood supply to hepatocellular carcinoma: angiographic demonstration and transcatheter arterial chemoembolization. Cardiovasc Intervent Radiol 29:39–48
14. Chung JW, Kim HC, Yoon JH et al (2006) Transcatheter arterial chemoembolization of hepatocellular carcinoma: prevalence and causative factors of extrahepatic collateral arteries in 479 patients. Korean J Radiol 7:257–266
15. Miyayama S, Yamashiro M, Okuda M et al (2009) Anastomosis between the hepatic artery and the extrahepatic collateral or between extrahepatic collaterals: observation on angiography. J Med Imaging Radiat Oncol 53:271–282
16. Takeuchi Y, Arai Y, Inaba Y et al (1998) Extrahepatic arterial supply to the liver: observation with a unified CT and angiography system during temporary balloon occlusion of the proper hepatic artery. Radiology 209:121–128
17. Uflacker R (1997) Atlas of vascular anatomy: angiographic approach. Williams & Wilkins, Baltimore, p 418
18. Lim JH, Kim B, Auh YH (1998) Anatomical communications of the perirenal space. Br J Radiol 71:450–456
19. Miyayama S, Yamashiro M, Okuda M et al. (2009) Hepatocellular carcinoma supplied by the right lumbar artery. CardioVasc Intervent Radiol (in press)
20. Head HW, Dodd GD III, Dalrymple NC et al (2007) Percutaneous radiofrequency ablation of hepatic tumors against the diaphragm: frequency of diaphragmatic injury. Radiology 243:877–884
21. Yamakado K, Nakatsuka A, Takai H et al (2008) Early-stage hepatocellular carcinoma: radiofrequency ablation combined with chemoembolization versus hepatectomy. Radiology 247:260–266
22. Kang TW, Rhim H, Kim EY et al (2009) Percutaneous radiofrequency ablation for the hepatocellular carcinoma abutting the diaphragm: assessment of safety and therapeutic efficacy. Korean J Radiol 10:34–42
23. Takaki H, Yamakado K, Nakatsuka A et al (2009) CT-guided RF ablation combined with chemoembolization for subphrenic hepatocellular carcinoma. J Vasc Interv Radiol 20:S10

Hepatocarcinogenesis: Multistep Changes of Drainage Vessels at CT during Arterial Portography and Hepatic Arteriography—Radiologic-Pathologic Correlation[1]

Azusa Kitao, MD
Yoh Zen, MD
Osamu Matsui, MD
Toshifumi Gabata, MD
Yasuni Nakanuma, MD

Purpose: To clarify the changes that occur in drainage vessels of dysplastic nodules and hepatocellular carcinoma (HCC) during hepatocarcinogenesis by using computed tomography (CT) during arterial portography (CTAP) and CT during hepatic arteriography (CTHA), with histologic findings as the reference standard.

Materials and Methods: Institutional ethics committee approval and informed consent were obtained. According to the findings at CTAP and CTHA, 46 surgically resected hepatocellular nodules were classified into three types: type A (n = 18) (equivalent or decreased portal perfusion compared with background liver at CTAP, decreased arterial perfusion, and no corona enhancement [perinodular contrast material drainage] at CTHA), type B (n = 13) (no portal perfusion, increased arterial perfusion, and thin (≤2-mm) corona enhancement), or type C (n = 15) (no portal perfusion, increased arterial perfusion, and thick (>2-mm) corona enhancement). We compared the histopathologic features and microangioarchitecture between the types.

Results: Type A nodules histologically consisted of dysplastic nodules and well-differentiated HCC; type B and C nodules were moderately differentiated HCC. Replacing growth was commonly observed in type A nodules, whereas compressing growth was more frequently seen in types B and C. Sixty percent of type C nodules had a fibrous capsule. There were significantly fewer intranodular hepatic veins in types B and C. Serial pathologic slices demonstrated continuity from intranodular capillarized sinusoids to hepatic veins in type A nodules and to surrounding hepatic sinusoids in type B nodules. In type C nodules, intranodular capillarized sinusoids were connected to extranodular portal veins either directly or through portal venules within the fibrous capsule.

Conclusion: Drainage vessels of HCC change from hepatic veins to hepatic sinusoids and then to portal veins during multistep hepatocarcinogenesis.

[1] From the Departments of Radiology (A.K., O.M., T.G.) and Human Pathology (A.K., Y.Z., Y.N.), Kanazawa University Graduate School of Medical Science, 13-1 Takaramachi, Kanazawa 920-8640, Japan. Received August 10, 2008; revision requested September 24; revision received January 7, 2009; accepted March 2; final version accepted March 16. Supported in part by Grant-in-Aid for Cancer Research (no. 18S-01) from Ministry of Health, Labor, and Welfare and by Health and Labor Sciences Research Grants for Development of Novel Molecular Markers and Imaging Modalities for Earlier Diagnosis of Hepatocellular Carcinoma. **Address correspondence to** A.K. (e-mail: *kitao@rad.m.kanazawa-u.ac.jp*).

Hepatocellular carcinoma (HCC) is usually associated with chronic liver disease, especially chronic viral hepatitis and liver cirrhosis (1,2). HCC has been proved to develop by multistep carcinogenesis from a dysplastic nodule (DN), to early HCC (highly well-differentiated HCC), and finally to overt hypervascular HCC (moderately differentiated HCC) (3–10).

To understand the pathophysiology of HCC, especially in its early stage, the multistep changes in the blood supply of DNs and HCC have been well studied with radiologic techniques (11,12). Computed tomography (CT) during arterial portography (CTAP) and CT during hepatic arteriography (CTHA) are useful radiologic methods for evaluating in vivo dynamics of portal supply and arterial supply, respectively, in hepatic lesions (11–17). DNs show the same or mildly decreased portal perfusion at CTAP and decreased arterial perfusion at CTHA compared with surrounding liver parenchyma. On the other hand, moderately differentiated HCC shows no portal perfusion at CTAP and clearly increased arterial perfusion at CTHA. In brief, the inflow of nodules changes from a mainly portal supply to an exclusively arterial supply during the multistep hepatocarcinogenesis (12). These radiologic findings reflect the histologic vascular structure of HCC (18,19).

Advances in Knowledge

- The main drainage vessels of hepatocellular carcinoma (HCC) change from hepatic veins to hepatic sinusoids to portal veins during multistep hepatocarcinogenesis.
- The thickness of corona enhancement (perinodular drainage of contrast material) of HCC at late-phase CT during hepatic arteriography correlates with the histologic grade of tumor malignancy and the type of drainage vessels.
- The changes in HCC drainage vessels could be triggered by the early reduction of intranodular hepatic veins owing to tumor invasion.

In comparison to inflow, little attention has been paid to drainage flow of HCC and DNs, although a few radiologic studies regarding drainage vessels of HCC have been published (20–22). Ueda et al (22) used single-level dynamic CTHA to clarify the drainage vessels of hypervascular HCC with a fibrous capsule. In their study, intranodular contrast enhancement was observed, and subsequently, perinodular enhancement with bright branching structures appeared on single-level dynamic CTHA images. They concluded that perinodular enhancement, named *corona enhancement*, is the drainage area of the tumor and that the branching structures are portal venules corresponding to the drainage route. However, the radiologic-pathologic correlation has not been fully elucidated. In particular, how the drainage vessels change during multistep hepatocarcinogenesis has not been examined.

In our study, we tried to clarify the changes that occur in drainage vessels during hepatocarcinogenesis from DN to moderately differentiated HCC. We evaluated intranodular and perinodular hemodynamics by using CTAP and CTHA, with a focus on the correlation of corona enhancement at late-phase CTHA with histopathologic features.

Materials and Methods

Patients

This retrospective study was performed with the approval of the institutional ethics committee, and informed consent was obtained from patients. It focused on 46 hepatocellular nodules in 40 patients, which were surgically resected and were pathologically diagnosed as DNs or HCC at our institution between 1998 and 2007. We did not include large (>6 cm in diameter) nodules or poorly differentiated HCCs, because they are often associated with secondary changes that might influence imaging (eg, necrosis, hemorrhage, invasion of the portal or hepatic veins). All patients (mean age, 61.0 years ± 8.4 [standard deviation]; men, 85%; women, 15%) had chronic liver disease. No patient had previously undergone treatment (eg, ablation therapy, transarterial chemoembolization therapy, chemotherapy) for hepatocellular nodules.

Implications for Patient Care

- The grade of tumor malignancy may be indicated by analyzing corona enhancement of HCC at dynamic CT, dynamic MR imaging, or contrast-enhanced US.
- Knowledge of venous drainage is important for understanding the pathophysiology of HCC and for precise performance of interventional therapy or surgical resection.

CTAP and CTHA

Both CTAP and CTHA were performed in all patients before surgical resection (mean time before surgery, 41.3 days ± 17.8) because of their extremely high sensitivity for detection of other nodular lesions (11). CTAP and CTHA were performed with various CT scanners (XVision SP, Toshiba Medical Systems, Tokyo, Japan; Aquilion 64, Toshiba Medical Systems; HiSpeed Advantage, GE Healthcare, Milwaukee, Wis; and LightSpeed Ultra 16, GE Healthcare). From the femoral artery, 4-F catheters were inserted into the superior mesenteric artery for CTAP and into

Published online
10.1148/radiol.2522081414

Radiology 2009; 252:605–614

Abbreviations:
CTAP = CT during arterial portography
CTHA = CT during hepatic arteriography
DN = dysplastic nodule
HCC = hepatocellular carcinoma

Author contributions:
Guarantors of integrity of entire study, all authors; study concepts/study design or data acquisition or data analysis/interpretation, all authors; manuscript drafting or manuscript revision for important intellectual content, all authors; approval of final version of submitted manuscript, all authors; literature research, A.K., O.M.; clinical studies, A.K., Y.Z., O.M., T.G., Y.N.; statistical analysis, A.K.; and manuscript editing, A.K., Y.Z., O.M., Y.N.

Authors stated no financial relationship to disclose.

the common, proper, or replaced right hepatic artery for CTHA.

CTAP scans were obtained at 5–7-mm section thickness and 5–7-mm collimation to cover the entire liver in a single breath hold. To increase the blood flow and decrease the laminar flow of the portal vein, 5 μg of prostaglandin E1 (Palux; Taisho, Tokyo, Japan) was injected into the superior mesenteric artery before contrast material infusion. Helical scanning began 25 seconds after the infusion of 50–70 mL of iohexol (320–350 milligrams of iodine per milliliter) (Omnipaque; Daiichi, Tokyo, Japan) at a rate of 1.8 mL/sec by using a power injector was started.

CTHA scans were obtained at 3–5-mm section thickness and 3–5-mm collimation. Helical scanning was started 7 seconds after the beginning of an infusion of iohexol (320–350 milligrams of iodine per milliliter) into the common, proper, or replaced hepatic artery at a rate of 1.8 mL/sec. The infusion of contrast material was continued until 5 seconds after early-phase CTHA scanning was completed. The scanning time varied according to the individual liver size (about 20–25 seconds). The total amount of contrast medium varied according to the following equation: (early-phase scanning time + 12 seconds) × injection rate. Thirty seconds after contrast material infusion finished (about 62–67 seconds after the infusion began), late-phase scanning commenced.

Radiologic Classification of Hepatocellular Nodules

The nodules were retrospectively classified into three types according to the findings at CTAP and CTHA in consensus by two radiologists (A.K. and O.M., with 8 and 38 years experience, respectively) who were blinded to any pathologic information. The classifications were determined on the basis of past reports about the findings of CTAP and CTHA.

We defined a type A nodule as a nodular lesion that showed equivalent or decreased portal perfusion as compared with background liver on CTAP images, decreased arterial perfusion compared with background liver on early-phase CTHA images, and no perinodular stain-

Figure 1

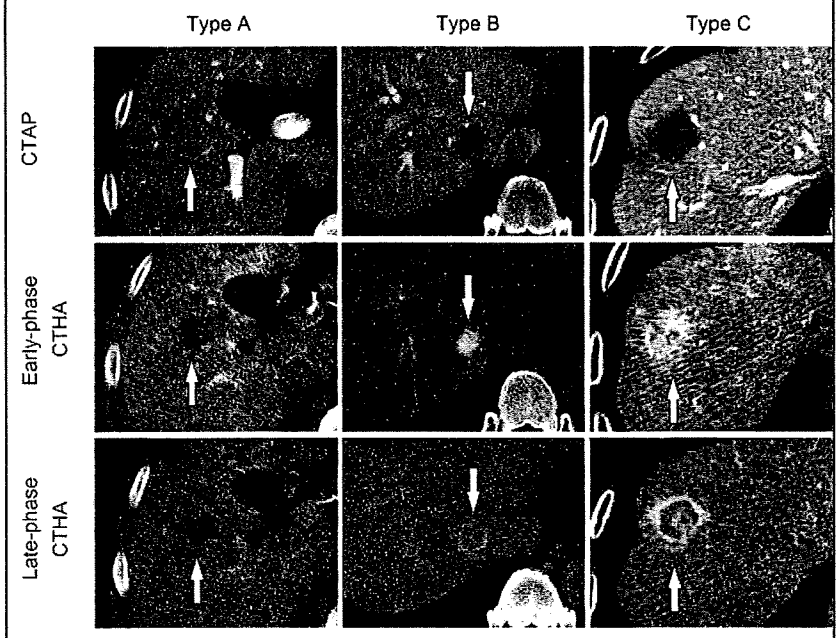

Figure 1: Typical CTAP (top row), early-phase CTHA (middle row), and late-phase CTHA (bottom row) findings for the three nodule types (arrows). Type A nodule (left column) has equivalent-to-decreased portal perfusion on CTAP imaging, decreased arterial perfusion on early-phase CTHA images, and no corona enhancement on late-phase CTHA images. Type B nodule (middle column) has portal perfusion defect and increased arterial perfusion with thin corona enhancement. Type C nodule (right column) has portal perfusion defect, increased arterial perfusion, and thicker corona enhancement.

Clinical Features by Tumor Type

Clinical Feature	Type A	Type B	Type C
No. of tumors	18	13	15
Resected tumor size (cm)*	2.0 ± 1.2 (0.9–4.8)	2.7 ± 1.6 (1.2–5.2)	2.6 ± 1.2 (1.6–5.5)
Age (y)*	58.9 ± 6.6 (47–70)	62.6 ± 8.9 (53–71)	62.7 ± 9.6 (53–76)
Male-to-female ratio	14:4	10:3	14:1
Underlying disease process			
Chronic hepatitis	6	3	6
Hepatitis B virus	2	0	1
Hepatitis C virus	4	3	4
Hepatitis B and C viruses	0	0	1
Liver cirrhosis	12	10	9
Hepatitis B virus	3	4	5
Hepatitis C virus	7	5	3
Cryptogenic	2	1	1

Note.—Unless otherwise specified, data are numbers of patients.

* Data are means ± standard deviations, with ranges in parentheses.

ing corona enhancement on late-phase CTHA images. Type B nodules showed no portal perfusion, clearly increased arterial perfusion compared with background liver, and thin corona enhancement. Thin corona enhancement was defined as flat perinodular enhancement on late-phase CTAP images that was less than or equal to 2 mm thick. Type C nodules showed no portal perfusion, clearly increased arterial perfusion compared with background liver, and thick corona enhancement on late-phase CTHA images. Thick corona enhancement was defined as perinodular enhancement with or without irregular protrusions that was greater than 2 mm thick. We set this 2-mm threshold because we clinically observed that smooth or flat corona enhancement was exclusively less than 2 mm thick, and in contrast, irregular or protruding corona enhancement was almost always more than 2 mm thick.

Type A nodules corresponded to DNs or well-differentiated HCCs, and type B and C nodules were part of well-differentiated HCCs or, mainly, moderately differentiated HCCs (11–17). There was no case that showed apparent reduction of portal perfusion of the liver on CTAP images. Typical CTAP and CTHA findings for the three types of nodules are shown in Figure 1.

Pathologic Examinations

Liver specimens were fixed with neutral formalin, and 4-mm-thick paraffin-embedded tissue slices were prepared from each nodule. Hematoxylin-eosin staining was performed. To clearly differentiate each vessel, double immuno-

Figure 2

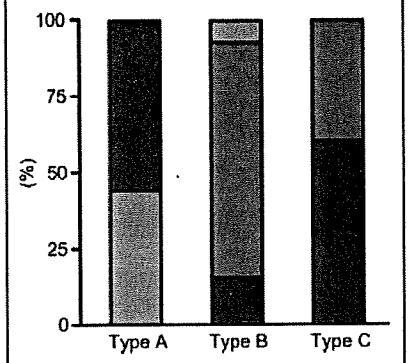

Figure 2: Bar graph of percentage of each tumor differentiation grade by tumor type. Blue = DN ($n = 10$), green = well-differentiated HCC ($n = 9$), orange = moderately differentiated HCC without fibrous capsule ($n = 16$), red = moderately differentiated HCC with fibrous capsule ($n = 11$).

Figure 3

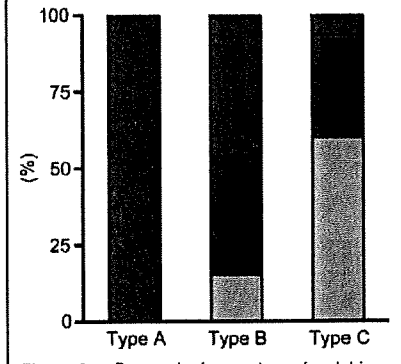

Figure 3: Bar graph of percentage of each histologic growth pattern by tumor type. Blue = replacing growth, red = compressing growth without fibrous capsule, green = compressing growth with fibrous capsule.

Figure 4

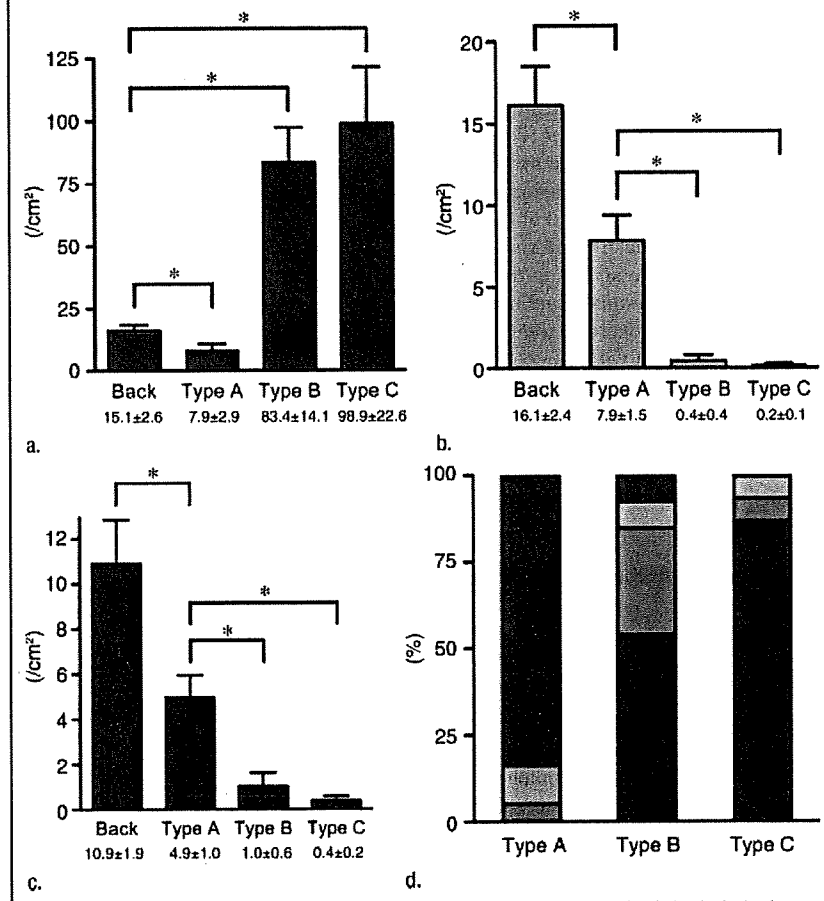

Figure 4: Bar graphs of density of intranodular vessels by nodule type compared with that in the background liver tissue *(Back)* for **(a)** arteries, **(b)** portal vein, and **(c)** hepatic vein. Mean value ± standard deviation is given under each bar. * = $P < .05$ with multiple comparison test. **(d)** Bar graph of percentage of area of capillarized sinusoids by nodule type shows progressive increase in percentage of capillarized area in type A versus type B versus type C nodules ($P < .05$ with Kruskal-Wallis test). Blue = 1+, green = 2+, orange = 3+, red = 4+.

Figure 5

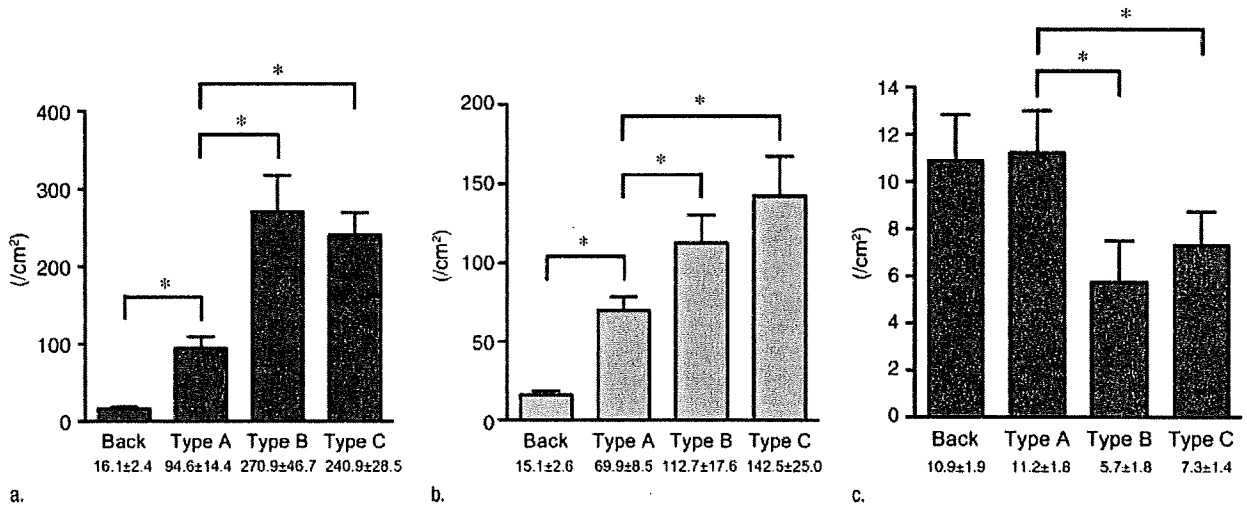

Figure 5: Bar graphs of density of perinodular vessels by nodule type compared with that in the background liver tissue *(Back)* for **(a)** arteries, **(b)** portal vein, and **(c)** hepatic vein. Mean value ± standard deviation is given under each bar. * = $P < .05$ with **(a, b)** multiple comparison or **(c)** unpaired *t* test.

staining with CD34 (a vascular endothelial cell marker) and α–smooth muscle actin (a smooth muscle cell marker) was performed in all nodules. Two pathologists (Y.Z. and Y.N., with 11 and 37 years experience, respectively) and one radiologist (A.K.), who were blinded to all imaging information, evaluated the three nodule types in consensus for tumor differentiation, fibrous capsule formation, tumor growth pattern, background liver tissue (chronic hepatitis or liver cirrhosis), and number of vessels.

Tumor differentiation and fibrous capsule.—We classified each nodule into one of four grades for tumor differentiation according to the classifications proposed by the International Working Party (8) and the World Health Organization (23): DN, well-differentiated HCC, moderately differentiated HCC without fibrous capsule, and moderately differentiated HCC with fibrous capsule. A DN was defined as a small nodular lesion of hepatocytes with mild nuclear and cytoplasmic atypia, cellular density increase, and no evidence of malignancy (eg, stromal or vessel invasion). In our study, the DN category included both low- and high-grade DNs because they both show similar findings on CTAP and CTHA images (17). Well-differentiated HCC was de-

Figure 6

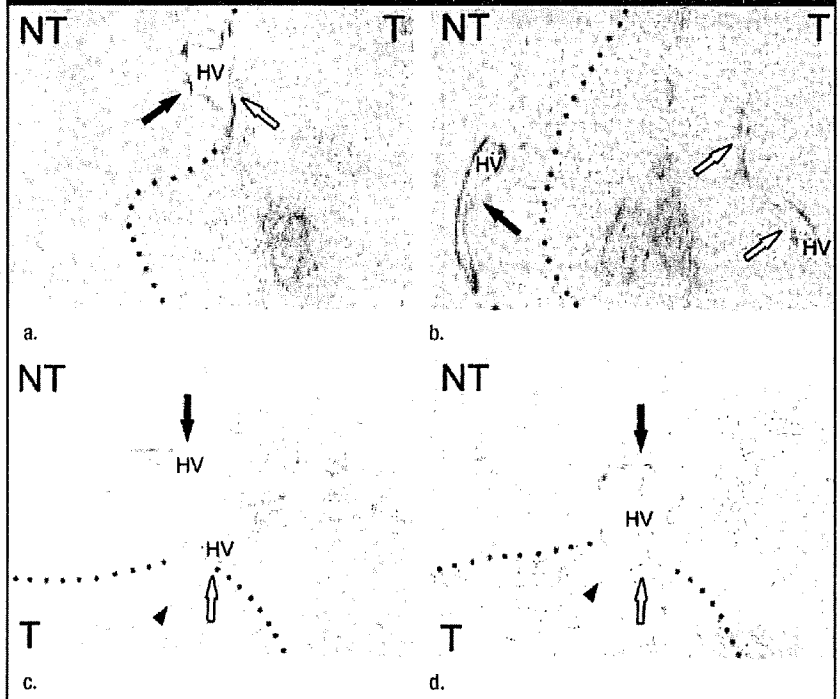

Figure 6: Serial pathologic slices show continuity of vessels at the border (dotted line) of a type A nodule (DN). **(a, b)** Intranodular preexisting hepatic vein (*HV*, white arrows) and extranodular hepatic veins (black arrows). **(c, d)** Intranodular capillarized sinusoid (arrowheads) continues into hepatic vein (white arrows) at nodule border and then into extranodular hepatic vein (black arrows). *NT* = not tumor, *T* = tumor. (Double immunostaining with CD34 [brown] and α–smooth muscle actin [red]; magnification, ×200.)

Figure 7

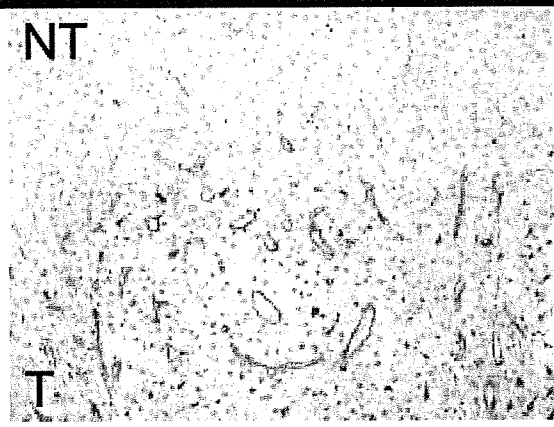

Figure 7: Continuities of intranodular capillarized sinusoids (brown) and extranodular hepatic sinusoids are diffusely observed at the border of a type B nodule (moderately differentiated HCC with replacing growth). *NT* = not tumor, *T* = tumor. (CD34 and α–smooth muscle actin; magnification, ×200.)

Figure 8

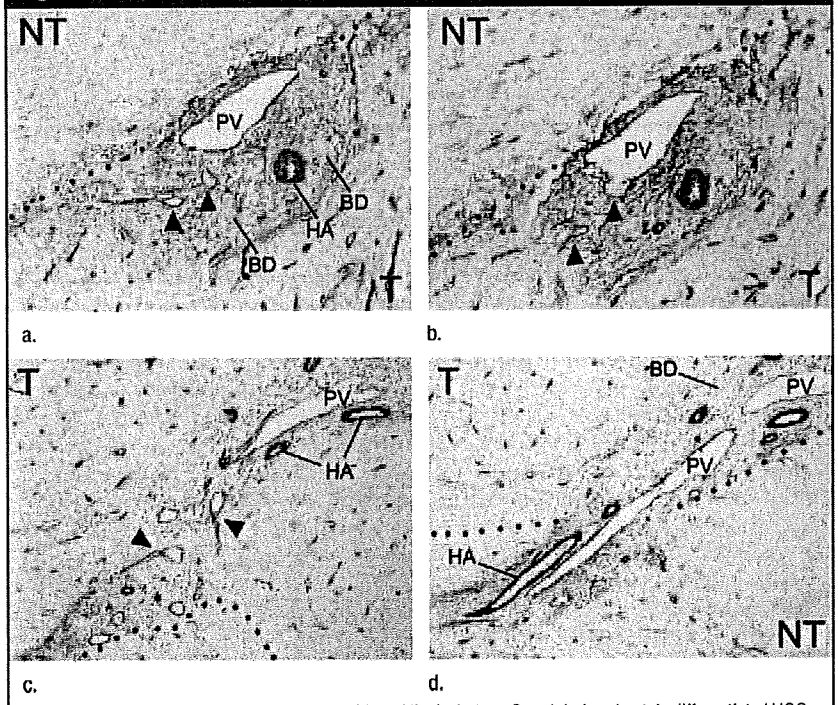

Figure 8: Continuities of vessels at border (dotted line) of a type C nodule (moderately differentiated HCC without fibrous capsule). Intranodular capillarized sinusoids (arrowheads) connect to extranodular portal veins *(PV)* **(a, b)** directly and **(c, d)** indirectly (through portal venules within the fibrous septum). Portal venules are accompanied by hepatic arteries *(HA)* and bile ducts *(BD)*. *NT* = not tumor, *T* = tumor. (CD34 and α–smooth muscle actin; magnification, ×200.)

fined as a nodular lesion consisting of malignant hepatocytes that showed evident nuclear and cytoplasmic atypia and higher cellular density. Intranodular portal tracts were relatively preserved. Moderately differentiated HCC was composed of malignant hepatocytes proliferating in trabecular, pseudoglandular, and solid patterns. We defined a fibrous capsule as fibrous tissue that was greater than 0.2 mm thick and surrounded more than two-thirds of the tumor circumference.

Tumor growth pattern.—Nodule growth patterns were classified into two types: replacing and compressing. In the nodules with replacing growth, tumor cells proliferated by replacing surrounding hepatic parenchyma, and the margin between nodules and background liver tissue was indistinct. Compressing-growth nodules had a discrete margin and pushed out the surrounding hepatic parenchyma.

Underlying disease process.—For each nodule type, we compared the proportion of patients with chronic hepatitis with that of patients with liver cirrhosis to analyze the influence of the underlying disease process on background liver tissue.

Number of vessels.—We counted the numbers of vessels twice. The number of arteries (both hepatic and neovascularized unpaired arteries), portal veins, and hepatic veins were counted in three areas: within tumor parenchyma, not including the fibrous septa or fibrous capsule; in the perinodular area less than 2 mm from the nodule border; and in the background liver away from the nodule. Intranodular and background liver vessels were counted in the largest square we could draw in the respective areas of the tissue slices. Perinodular vessels were counted in 10 random fields within 2 mm of the tumor border (magnification, ×100) or within as many fields as possible on small slices. Then, we divided the number of vessels by the area to calculate vessel density (per square centimeter).

We also measured the area of intranodular capillarized sinusoids covered by endothelial cells expressing CD34 and compared it with the whole

area of the nodule in the same slice (18,24). Capillarized area in each nodule was semiquantitatively rated as follows: 1+ = 0%–25%, 2+ = 26%–50%, 3+ = 51%–75%, and 4+ = 76%–100%.

Continuity of vessels at nodule border.—To clarify the continuity between intranodular vascular structures and extranodular drainage vessels at the border of the nodule, more than 200 serial slices were prepared from one tumor of each type (ie, A, B, and C). By using double immunostaining with CD34 and α-smooth muscle actin, we examined continuities between intranodular and extranodular vascular structures on serial slices.

Statistical Analysis

The data were expressed as means ± standard deviations. Statistical significance was evaluated by using the Kruskal-Wallis test for the comparison of tumor differentiation, tumor growth pattern, and the area of intranodular capillarized sinusoids; unpaired *t* test for the comparison of the number of perinodular hepatic veins between tumor types; and multiple comparison test (Dunnet procedure) for the analysis of the number of other vessels. *P* values less than .05 were considered to indicate statistical significance.

Results

Clinical Features by Nodule Type

Eighteen nodules were classified as type A; 13, as type B; and 15, as type C. The clinical features of the patients and the tumor sizes are listed by type in the Table. As determined from resected specimens, the mean size of all hepatocellular nodules was 2.4 cm ± 1.3.

Pathologic Features by Nodule Type

Tumor differentiation and fibrous capsule.—At histologic analysis (Fig 2), type A nodules consisted of 10 DNs and eight well-differentiated HCCs. Type B nodules comprised one well-differentiated HCC and 12 (92%) moderately differentiated HCCs, 10 (83%) of which did not have a fibrous capsule. All 15 type C nodules were moderately differentiated HCCs, nine (60%) of which had a fibrous capsule (Kruskal-Wallis test, $P < .05$).

Figure 9

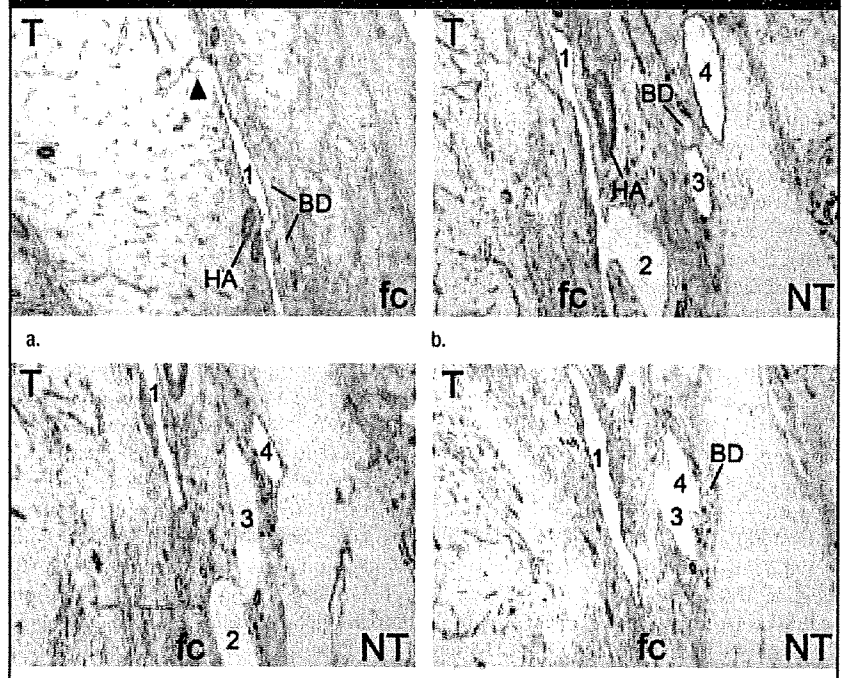

Figure 9: **(a–d)** Continuities of vessels at the border of a type C nodule (moderately differentiated HCC with fibrous capsule *[fc]*). Intranodular capillarized sinusoid (arrowhead, **a**) connects to portal venules (*1*, **a**) and drains into extranodular portal veins (*1–4*, **b–d**). *BD* = bile duct, *HA* = hepatic arteries, *NT* = not tumor, *T* = tumor. (CD34 and α-smooth muscle actin; magnification, ×100.)

Tumor growth pattern.—Histologic growth patterns for each type are shown in Figure 3. All of the type A nodules showed a replacing growth pattern. Half of type B nodules had replacing growth, and the other half had compressing growth. Almost all type C nodules (93%) showed compressing growth (Kruskal-Wallis test, $P < .05$). The proportion of nodules with compressing pattern was higher in type C than in type B (93% vs 54%).

Underlying disease process.—No significant difference with regard to histologic findings in the liver was observed between the three types of nodules. The percentages of chronic hepatitis and liver cirrhosis were 33% versus 67%, respectively, for type A nodules; 23% versus 77%, respectively, for type B nodules; and 33% versus 67%, respectively, for type C nodules.

Intranodular vessels.—Compared with the that in the background liver, the density of intranodular arteries was decreased in type A nodules and increased in type B and C nodules (all $P < .05$) (Fig 4). There was no statistically significant difference in the density of arteries between type B and C nodules. The density of intranodular portal veins was also decreased in type A nodules compared with the background liver and was decreased in type B and C nodules compared with type A nodules (all $P < .05$). The density of hepatic veins was similarly decreased ($P < .05$). The percentage of the nodule occupied by intranodular capillarized sinusoids progressively increased in type A versus B versus C nodules (Fig 4).

Perinodular vessels.—As shown in Figure 5, the density of perinodular arteries and portal veins was increased in type A nodules compared with the back-